metals

MDPI

Article

Development of Tool Wear Standards and Wear Mechanism for Micro Milling Ti-6Al-4V Alloy

Tao Zheng [1], Qinghua Song [1,2,*], Yicong Du [1,2] and Zhanqiang Liu [1,2]

[1] Key Laboratory of High Efficiency and Clean Mechanical Manufacture, Ministry of Education, School of Mechanical Engineering, Shandong University, Jinan 250061, China; 201913955@mail.sdu.edu.cn (T.Z.); duyicong@sdu.edu.cn (Y.D.); melius@sdu.edu.cn (Z.L.)

[2] National Demonstration Center for Experimental Mechanical Engineering Education, Shandong University, Jinan 250061, China

* Correspondence: ssinghua@sdu.edu.cn; Tel.: +86-(05)-3188392539

Abstract: With the rapid development of high-precision-device technology, new demands are put forward for micro milling. The size effect and low cutting energy of micro milling make the process expensive and difficult, especially for Ti-6Al-4V alloys. The wear of the micro-milling cutter lacks corresponding international standards and its cutting mechanism is complex. In this paper, four kinds of micro-milling cutters with different wear states were obtained by designing micro-milling experiments, and the wear process and wear mechanism were observed and analyzed. The cutter diameter reduction, end face wear, flank wear and edge radius are comprehensively analyzed. It is considered that the formulation of a micro-milling-cutter wear standard needs comprehensive consideration, and the wear of end face 30 μm, wear of flank 35 μm and tool diameter reduction 55 μm can be used as the failure criteria of the micro-milling cutter. The wear forms mainly include abrasion marks, material adhesion, built-up edges and micro-collapse blades. Adhesive wear exists in the whole cutting process and plays a major role. Abrasive wear, diffusion wear and oxidation wear will occur when the cutting temperature reaches the melting point of Co. The wear of the micro-milling cutter is analyzed more comprehensively, a new wear-failure standard is formulated and the complex wear mechanism is revealed.

Keywords: micro-milling-cutter wear; wear standard; wear form; wear mechanism

check for updates

Citation: Zheng, T.; Song, Q.; Du, Y.; Liu, Z. Development of Tool Wear Standards and Wear Mechanism for Micro Milling Ti-6Al-4V Alloy. *Metals* **2022**, *12*, 726. https://doi.org/10.3390/met12050726

Academic Editors: Tadeusz Mikolajczyk, Danil Yurievich Pimenov and Munish Kumar Gupta

Received: 25 March 2022
Accepted: 20 April 2022
Published: 24 April 2022

Publisher's Note: MDPI stays neutral with regard to jurisdictional claims in published maps and institutional affiliations.

Copyright: © 2022 by the authors. Licensee MDPI, Basel, Switzerland. This article is an open access article distributed under the terms and conditions of the Creative Commons Attribution (CC BY) license (https://creativecommons.org/licenses/by/4.0/).

1. Introduction

Micro milling has the advantages of high material removal rate, flexible processing technology, low installation cost and wide application range [1]. From macro processing to micro processing, some neglected problems in macro processing play an important role, such as the size effect, poor surface finish, upper milling burr, lower milling burr, minimum chip thickness, shortening tool life, rapid tool fracture [2], etc. When the workpiece material has difficulty cutting metal alloy, the difficulty of micromachining increases greatly. The low specific cutting energy limits the application of micro milling in the field of titanium alloy [3,4]. Titanium alloy is widely used in biomedicine, aerospace, electric power, ocean, automobile and other industries [5,6] because of its high strength–weight ratio, low density, high corrosion resistance and high biocompatibility [7]. Although titanium alloy has these superior properties, its poor thermal conductivity, high friction coefficient and reduced wear resistance limit the application of titanium alloy [8]. Poor thermal conductivity leads to high cutting temperature, adhesion between workpiece material and tool cutting surface, shortened tool life, obvious chips and premature failure of the cutting-edge radius [9].

One of the main challenges of micro milling is the understanding of the process of tool wear and breakage and its mechanism. These processes are usually different from those observed in traditional milling operations. The definition and prediction of conventional macro-milling life is prescribed by the ISO-8688 standard (part first and part second) [10,11],

which does not involve micro milling. Therefore, the research on the wear state of the micro-milling cutter is lacking relevant international standards. In the process of micro milling, there are some phenomena that cannot be observed by conventional milling, such as size effect, minimum chip thickness and blade radius [12]. In micromachining, the edge radius becomes more important than the thickness of the removed material, and they are at the same micron level. If the uncut chip thickness is less than the critical value, i.e., the minimum chip thickness [13], it will not be cut, but will produce a plowing effect. The establishment of criteria to evaluate the wear of the cutting edge in micro milling is challenging. Zhu and Yu [14] proposed a wear-area-analysis method based on the top images of worn tools. It was observed that the wear area was triangular and the area gradually expanded. Alhadeff et al. [15] emphasized that the edge radius, end face wear length and flank wear length are three key parameters when developing the wear-measurement standard of a micro-milling cutter, which can quantitatively measure and evaluate progressive tool wear. Han et al. [16] carried out a micro-milling experiment on oxygen-free copper with a PCD (polycrystalline diamond) tool and selected a cemented-carbide micro-milling cutter in the comparative experiment. Through the parameter test, the variation laws of milling force and specific energy are analyzed, and the surface quality, machining accuracy and tool wear are further studied. Manso et al. [17] studied the model of tool diameter reduction caused by tool wear during the micro milling of H13 tool steel. Ziberov et al. [18] developed a method to measure two different types of flank wear by comparing new and old tools. They put the Ti-6Al-4V tool at a diameter of 152.4 μm. The end-life criterion for micro milling on uncoated cemented-carbide tools of M is defined as 10 μm. In the experimental observation of tool wear patterns in the Ti-6Al-4V micro-milling process, Dadgari et al. [19] identified three stages: rapid initial wear, gradual but uneven wear expansion and final accelerated wear. For the tool with a diameter of 1 mm, the failure criteria of 37.5 μm rear tool surface wear, 33 μm edge radius and 1 μm average surface roughness are proposed. Compared with the traditional tool wear, the wear of a macro-milling cutter mainly occurs on the flank, and the wear of a micro-milling cutter occurs not only on the flank, but also on the tip and tool diameter. The wear standard of the traditional milling cutter is no longer applicable to a micro-milling cutter. Therefore, the formulation of a micro-milling-cutter wear standard needs comprehensive consideration and analysis.

Although there are many reports on the research of tool wear in macro machining, there is little research on the formulation of a tool-wear standard in micro end milling. At present, there is still a lack of international wear standards and systematic wear mechanism research of micro-milling cutters. During groove milling of stainless steel using 800 μm tungsten carbide tools, Oliaei and Karpat [20] emphasized that tool wear evolved primarily through the cutting radius and back face wear. Silva et al. [21] studied the machinability and wear behavior of micro-cutting teeth with a scanning electron microscope and X-ray energy spectrometer. It proved that the high adhesion of a diamond coating can be achieved by the appropriate combination of chemical erosion and coating structure. Muhammad et al. [22] used optical profilometer, scanning electron microscope and statistical techniques for analysis. The research determined that the cutting depth is the main factor affecting the formation of burr, and the cutting speed is the main factor affecting the surface roughness. To investigate the influence of tool wear on machinability in micro milling Ti-6Al-4V using Ti(C7N3)-based ceramic tools, Wang et al. [23] briefly mentioned that attachment, accumulation edge formation and micro-fracture edge are the main modes of tool wear. The influence of tool wear on cutting performance is studied, but the development process of tool wear is not discussed in detail. However, Sahoo et al. [24] found that the coating increases the edge radius of the tool, which increases additional plowing and friction. Varghese et al. [25] emphasized the difficulty of understanding tool wear patterns and the fact that a micro-fracture edge is the most important wear type of a 500 μm diameter WC (wolframium carbide) micro-milling cutter in the process of machining stainless steel. Suha et al. [26] comprehensively and systematically analyzed the conditions of the blade

and chip during the wear process and revealed the wear mode and mechanism of coated-tool micro milling. They found that the edge radius increases with the increase of machining time, and the corresponding minimum uncut chip thickness also increases accordingly. The types of tool failures mainly include abrasion wear, dissolution and diffusion wear and chemical wear [27,28]. Thakur DG et al. [29] found that the main cause of accelerated tool wear was the change in the composition of Inconel718's front tool face and proposed the thermal softening and diffusion of these materials and the thermal mechanism of cutting super alloys. Gao Q et al. [30] conducted micro-milling experiments on single crystal nickel-based super alloy, analyzed wear mechanism and wear form by means of a scanning electron microscope (SEM) and energy-dispersive X-ray spectroscopy (EDS), and proposed the influence of tool and workpiece material element changes on workpiece performance in the cutting process. From a theoretical point of view, Zhang et al. [31] established the first chip-surface formation process model considering the strain gradient plasticity theory, deduced the equation of the minimum uncut thickness of chips, and established a micro-machined surface roughness model considering the influence of tool wear. Aslantas et al. [32] verified the mechanical model through a Ti-6Al-4V alloy test, indicating that the cutting depth and feed value are selected according to the edge radius. This shows the importance of the edge radius in micro cutting.

Compared with traditional cutting, the tool-wear mechanism in micro milling is more complex, the tool life is shorter, and it is difficult to observe and detect. The size effect determines the edge radius, which can no longer be ignored. Therefore, the study of tool wear in micro milling is of great scientific significance for tool selection, cutting-material process formulation and improving workpiece quality. In this paper, micro-milling cutters with different wear states were obtained through micro-milling experiments. The wear process, wear form and wear mechanism were analyzed by a confocal laser microscope, SEM (scanning electron microscope), EDS (energy dispersive spectrometer) and other means. In this paper, the tool diameter, end face wear, flank wear and edge radius of micro milling cutter are comprehensively analyzed. The establishment of a micro-milling cutter wear standard is attempted, and the comprehensive judging basis is put forward. The edge radius should be considered in micro milling, which is often ignored in traditional milling. The progressive normal wear failure and abnormal wear failure are analyzed and the wear mechanism is discussed. The formulation of a micro-milling wear standard and the disclosure of the wear mechanism are of great significance to its popularization and application.

2. Materials and Methods

The experimental work of this study was carried out on the self-developed high-speed micro-milling platform model BJEV-X\Y\Z-300\300\100. The digital optical confocal microscope VK-X200 (Keyence, Osaka, Japan) was used to obtain the 3D surface topography of the micro-milling cutter. The tool-diameter reduction, end-face wear and flank wear were also obtained by it. A field-emission high-temperature scanning electron microscopy JSM-7800F (JEOL, Tokyo, Japan) was used to obtain the micro-morphology of the tool surface. Combined with the obtained data information of the tool-end face and side, the change of the cutting-edge radius is comprehensively analyzed. We use EDS Oxford XMAX-80 (JEOL, Tokyo, Japan) to obtain the elemental spectra of the cutting tool and machining surface. The equipment used is shown in Figure 1.

The workpiece material is Ti-6Al-4V and the cutter is a φ1 tungsten-carbide micro-milling cutter without coating, which is the result of comprehensive consideration. The material chemistry of Ti-6Al-4V stock is shown in Table 1. The coating materials are generally TiN, TiCN, TiAlN, etc. Under the complex processing environment of high temperature and high pressure, high strain rate and thermal coupling, the titanium elements in the coating and the titanium elements in the workpiece easily produce element affinity, resulting in adverse consequences. At the same time, considering the influence of uncoated cutting tools without coating materials, it is easier to accurately explore the wear mechanism

between tool material WC and the workpiece material. The four-edge micro-milling cutter manufactured by Jiayi Seiko (Jiayi Seiko, Shenzhen, China) is adopted and the tool information is shown in Figure 2 and Table 2.

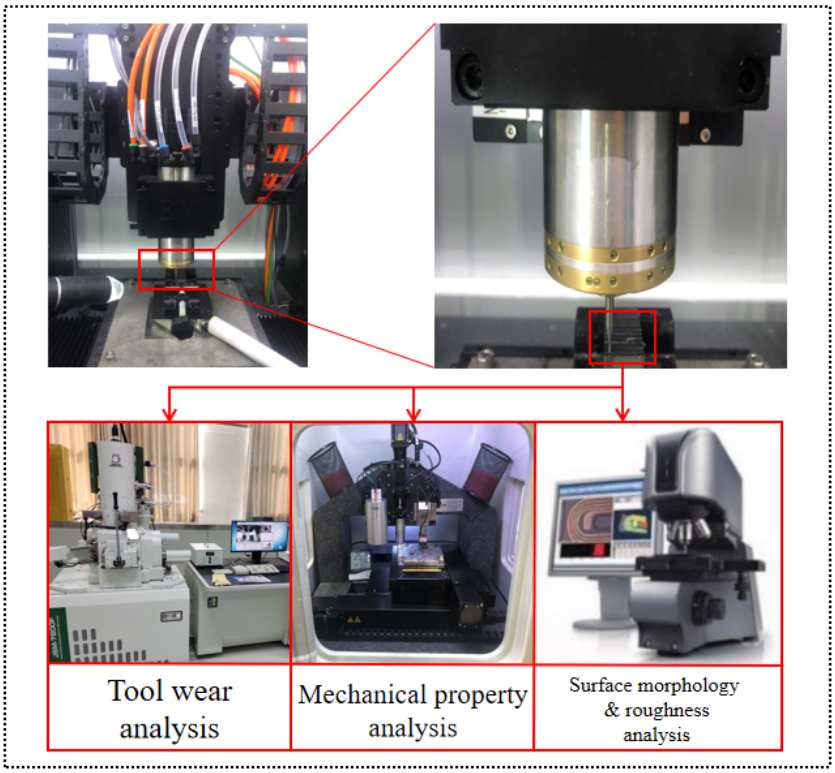

Figure 1. The experimental devices.

Table 1. The material chemistry of the Ti-6Al-4V stock.

Elements	Al	V	Fe	O	N	C	H	Ti
Content (Wt. %)	5.5	4.2	0.22	0.11	0.03	0.08	0.012	89.848

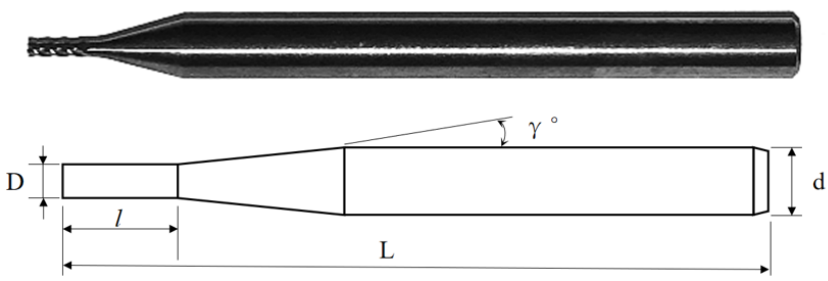

Figure 2. Micro-milling cutter and schematic diagram.

Table 2. Tool geometry data.

Cutting Edge Diameter (D)	Cutting Edge Length (*l*)	Cutter Length (L)	Tilt Angle (γ°)	The Handle Diameter (d)
1 mm	3 mm	50 mm	30	4 mm

First, the parameter comparison experiment is carried out, and the process parameters conducive to the machining surface quality are selected for research. According to the summary of experimental experience and literature reading, different speeds are selected for comparison. The speeds are 20,000 rpm, 25,000 rpm and 30,000 rpm. The cutting parameters are shown in Table 3. For single-factor analysis, the feed rate and cutting depth were maintained at 5 mm/min and 50 μm and comprehensively evaluate the roughness and burr size of the machined surface. The machined surfaces at different speeds photographed by the confocal microscope (Keyence, Osaka, Japan) shown in Figure 3a–c are machined surfaces of 20,000 rpm, 25,000 rpm and 30,000 rpm, respectively. It can be seen that the numbers and sizes of burrs at 30,000 rpm are small. The surface-roughness data are obtained through multi-file analysis software (VK-X Series, Keyence, Osaka, Japan). Under different processing parameters, the measurement area of burr shall be the place where the processing track coincides, because the burr is obvious here. The middle position of the processing path is uniformly selected for confocal laser image acquisition. The follow-up data are analyzed by VK software and collected five times to obtain the average value. Burr and roughness analysis are statistical methods to obtain the average value through multiple collection. After selecting the better machining parameters, the experimental plan adopts the control-variable method, which can better control the wear state of micro-milling tools. As shown in Figure 4, the roughness is the smallest at 30,000 rpm. To sum up, 30,000 rpm obtained the best machined surface quality, so the follow-up research was based on the rotating speed of 30,000 rpm.

Table 3. The cutting conditions.

Rotating Speed (n)	Feed Speed (V_f)	Cutting Depth (ap)
20,000/25,000/30,000 rpm	5 mm/min	0.05 mm

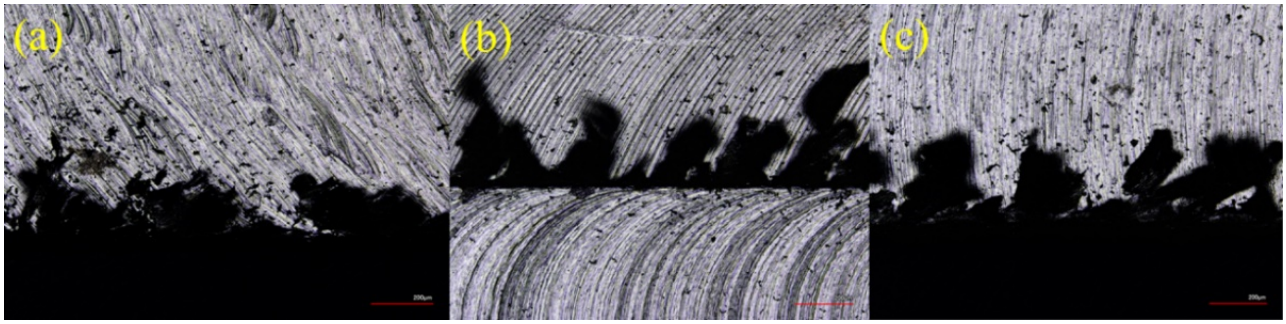

Figure 3. Machined surfaces with different machining parameters (**a**) n = 20,000 rpm, (**b**) n = 25,000 rpm, and (**c**) n = 30,000 rpm.

The experimental process is shown in Figure 5. In the figure, 0.05 mm represents the cutting depth, 5 mm × 4.6 mm represents the machining range, and n = 30,000 represents the rotating speed of 30,000 rpm. The parameter optimization experiment was carried out on a self-made micro-milling platform. From the above experimental data, it is found that the machining surface quality is better with the cutting speed of 30,000 rpm, the feed speed of 5 mm/min and the cutting depth of 50 μm, and the micro-milling cutter wear state is obviously distinguishable. Due to the size effect and the minimum chip thickness, the cutting effect is not good when the cutting depth is less than 50 μm, and the plowing phenomenon occurs easily. The evaluation method of micro-milling tool wear is complicated because of the change of machining mode and machining condition that are due to the small tool size, and there is no clear evaluation standard at present. Therefore, in this study, the reduction of tool diameter, the wear of the end face and the wear of the flank were selected to judge the wear state comprehensively. With the increase of material removal, the micro-milling cutter gradually wears away, so the machining length is used

to distinguish the cutter. The tool wear state was controlled by a single factor of material removal amount, and each milling plane (5 mm × 4.6 mm, with 0.1 mm overlap between machining paths) was cut, that is, machining 25 mm/50 mm/75 mm to distinguish different wear states. The processing direction adopts transverse turn-back processing to obtain the processing plane convenient for data acquisition. The plane is more conducive to data measurement. Initial/Wear I/Wear II/Wear III were used to represent the four wear states of the micro-milling cutter, and Initial was used to represent the original cutter. The wear degree of the latter three gradually increased. The surface was machined once (cutting 25 mm) with the new cutter and turned into Wear I. We used the tool of Wear I to process the primary surface to obtain Wear II and so on. Then four micro-milling cutters with different wear states were systematically studied.

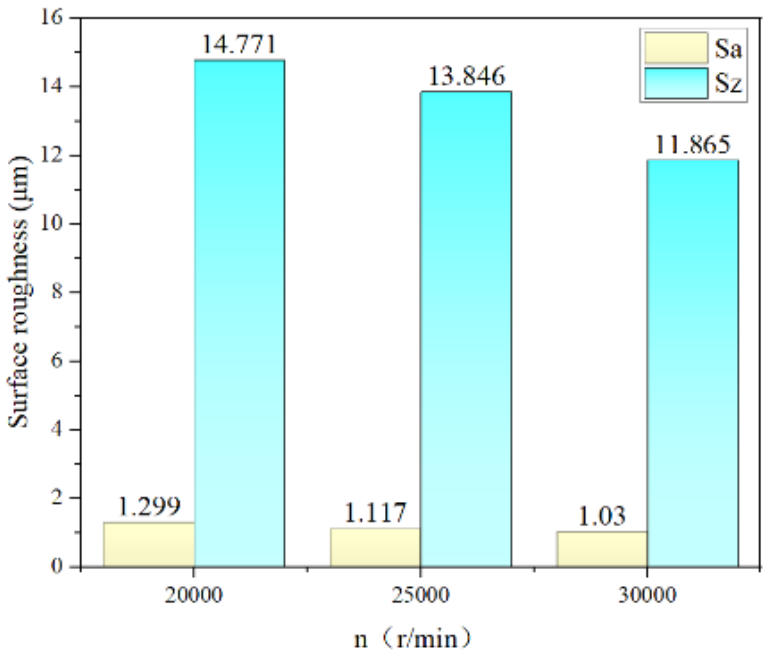

Figure 4. Surface roughness of different processing parameters.

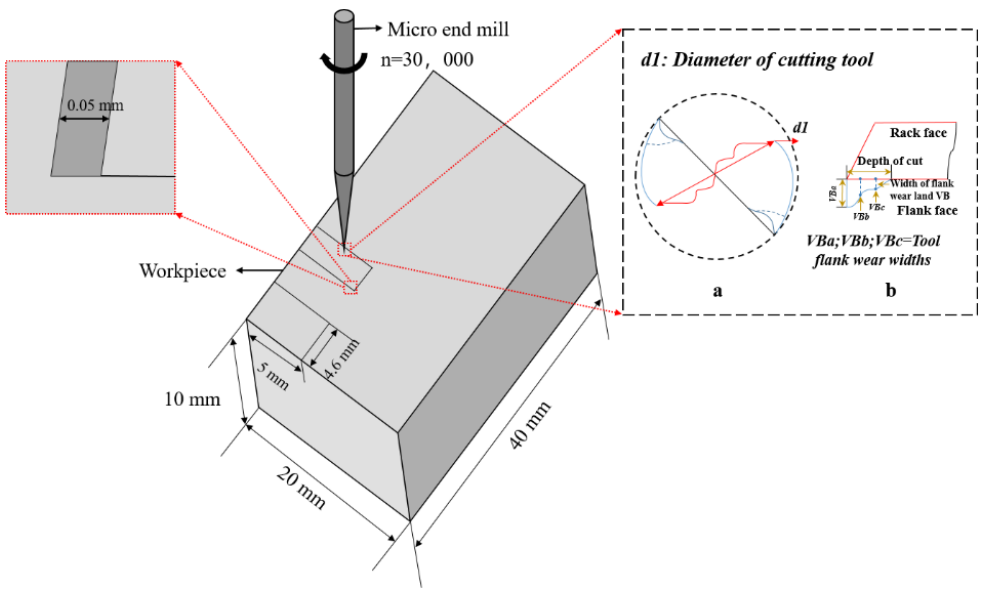

Figure 5. Schematic diagram of experimental scheme and geometrical measurement of wear (**a**) tool diameter reduction analysis and (**b**) wear analysis of rear tool face.

To study the wear process, wear form and wear mechanism of TI-6Al-4V milling with a WC carbide micro-milling cutter, it is necessary to have an understanding of deformation and heat propagation during the machining process. Figure 6 is a schematic diagram of the forming mechanism and heat generation of machined-surface integrity under the condition of tool wear. Because the cutting-edge radius and cutting depth are in the same order of magnitude, the size effect seriously affects the cutting performance of a micro-milling cutter. Therefore, the edge radius is highlighted in the schematic diagram. Micro milling is an environment of high temperature, high pressure and high strain rate. In this environment, micro-milling and machining surfaces are subjected to complex thermodynamic coupling effects, and complex chemical and physical changes occur under the dual influence of force and heat. The main shear zone (PDZ) is the area of chip formation, which mainly occurs in shear. It belongs to the elastic-plastic deformation affected by heat conduction and heat radiation in the extrusion process of the workpiece material. The tool chip friction zone (SDZ) mainly occurs in friction, which is a heating zone belonging to plastic deformation. It is affected by heat convection and heat dissipation and is in the tool chip interaction. The tool-work friction zone (TDZ) mainly occurs in friction, which is the formation area of the machining surface. It belongs to elastic deformation and is affected by thermal conduction and is located in the tool-work contact interaction area.

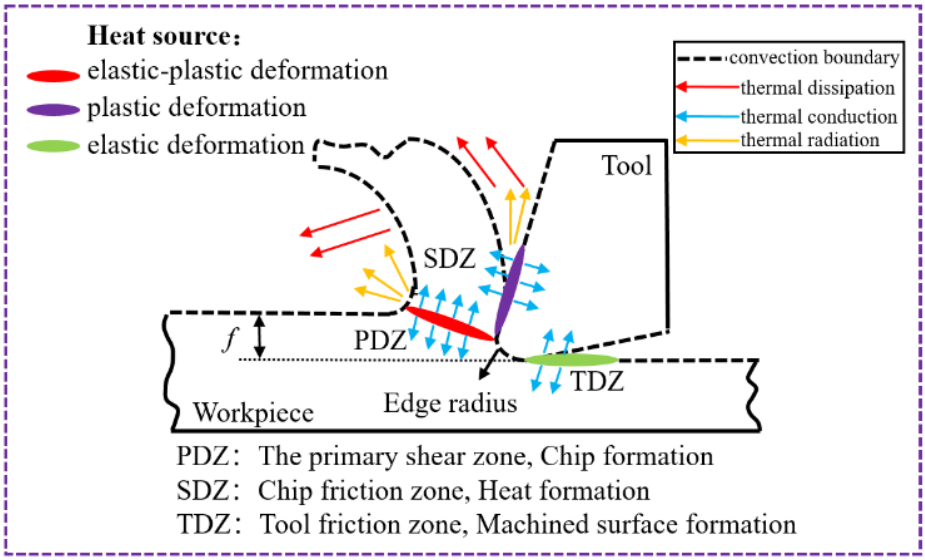

Figure 6. Mechanism and heat generation of machined surface integrity under tool wear conditions.

3. Results

3.1. End Face Wear

Confocal laser microscopy was used to photograph the end face of the micro-milling cutter. The end-face wear of each cutting edge was averaged by multi-point measurement, and then the data of four cutting edges were averaged again. Figure 7 is the C-Laser DIC form of the confocal microscopic image. In Figure 7, B1/B2/B3/B4 represent four cutting edges. The wear area of each cutting edge is marked with a yellow outline. (a), (b), (c) and (d) are Initial/Wear I/Wear II/Wear III, respectively. Due to tool wear, the phenomenon of tool-material spalling and micro-chipping occurs on the cutting edge, so the wear area is generated in the image. It can be seen that there is no wear in (a), and the wear area increases gradually with the deepening of the wear state, and the area in (d) reaches the peak, which is consistent with the fact that Wear III is the longest machining path and the most serious wear.

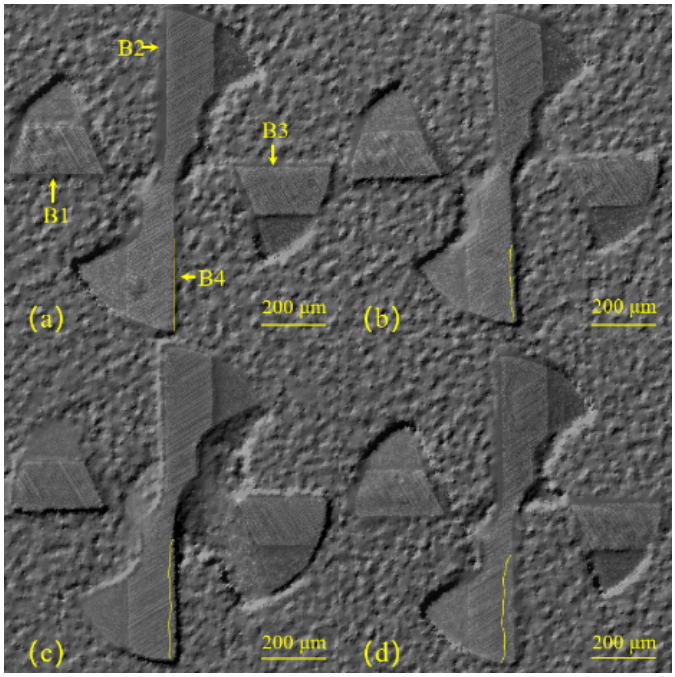

Figure 7. Schematic diagram of wear area of micro-milling cutter under different wear states.

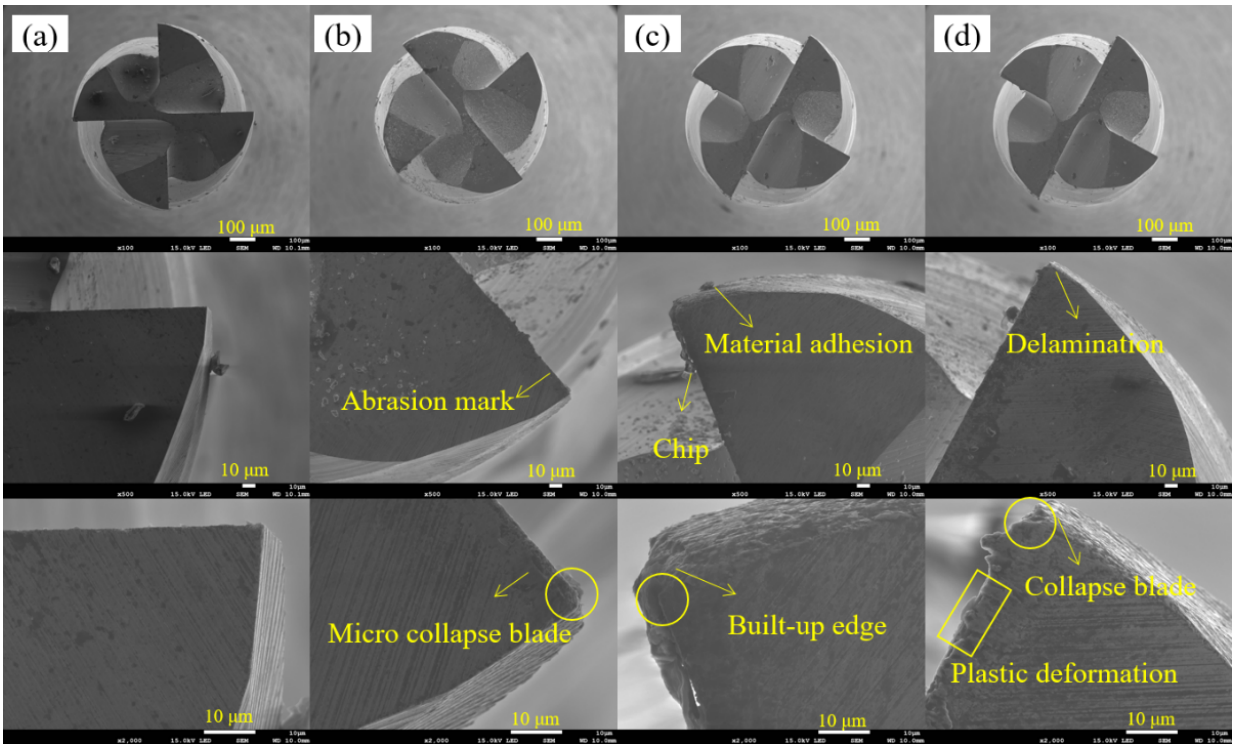

Figure 8. SEM image analysis of micro-milling cutter under different wear states. (**a**) Initial's 100/500/2000 × image, (**b**) Wear I's 100/500/2000 × image, (**c**) Wear II's 100/500/2000 × image, (**d**) Wear III's 100/500/2000 × image.

Figure 8 is the SEM image of a micro-milling cutter with different wear states. (a), (b), (c) and (d) are Initial/Wear I/Wear II/Wear III, respectively. Each row is a magnification factor, which is 100/500/2000 times in a turn. The wear modes are classified into progressive normal wear failure and abnormal wear failure. The progressive normal wear failure mainly includes abrasion marks, material adhesion, built-up edges (BUE) and micro-

collapse blades. The abnormal wear failure mainly includes severe plastic deformation, collapsed blades, catastrophic fractures and delamination of cutting edges. For the new cutter, the surface is extremely smooth because there is no wear. As the processing continues, Wear I has an abrasion mark and a micro-collapsed blade at the beginning. From the 500× image, it can also be seen that there are a few chips adhering to the cutting edge. The micro-milling cutter in Wear II has serious wear phenomena, and more chips attached to the cutting edge. In addition, in the 2000-times image, the formation of a stacking edge (BUE) is also obvious, especially on the flank face. BUE is the result of the bulk accumulation of workpiece material Ti-6Al-4V near the cutting edge, which is essentially the result of cold welding of the workpiece material near the cutting edge. During micro milling, the friction resistance between the chip friction zone (SDZ) and the tool is too large, and the material at the bottom of the chip will delay the slip. When the friction resistance is greater than the binding force of the chip material surface, Ti-6Al-4V will partially stop and adhere to the cutting edge, thus forming BUE. BUE will not be removed easily and will replace the cutting edge for cutting. As the chip will continue to supplement BUE as the cutting goes on and the hardness is large, it is beneficial for the cutting in the early stage. However, as processing time, this dynamically unstable structure changes in size and shape over time. Under the complex action of high-frequency load shock and vibration, the joint between the BUE and the cutting edge fatigues easily, and the BUE is easy to peel off. This causes part of the cutting edge to be taken away, which seriously affects the performance of the tool and reduces the quality of the machined surface. Therefore, the occurrence of BUE should be avoided, especially at the micro scale, where the adverse effects of BUE can be magnified. Different from progressive normal wear failure, abnormal wear failure refers to severe abnormal wear or fracture that causes the tool to lose its cutting ability. As for Wear III with the most serious wear degree, the wear area is further expanded and extended, the cutting edge is seriously worn, the shape and size change obviously, and the blade collapse phenomenon is more obvious. Compared with Wear II, BUE decreases, which is due to the further wear of the cutting edge as the cutting process continues. Part of BUE peels off under the dynamic action, resulting in part of the cutting edge being taken away. Therefore, under the long-term tool wear, the micro-milling cutter has the phenomenon of desquamating and blade collapse, which greatly reduces the cutting performance. In addition, the plastic deformation at the blade is serious, which is caused by the heat and stress concentration caused by the local high temperature in the cutting area, which also reduces the cutting performance.

3.2. Flank Wear

For traditional milling, the international standard stipulates that flank wear is the basis for judging the wear state of the milling cutter. Therefore, when analyzing the wear state of the micro-milling cutter, the flank-wear analysis is very necessary. Among the four cutting edges, B4 has the most obvious flank wear, so we focus on it. Figure 9 shows the wear images of the flank of the micro-milling cutter in different wear states taken by a confocal laser microscope, where (a), (b), (c) and (d), respectively, represent Initial, Wear I, Wear II and Wear III. The tool-wear area and contour are also marked in the figure. As shown in the figure, the new knife is smooth and flat, and the contour of the cutting edge is also angular. The wear area of the Wear I micro-milling cutter is small, and only slight wear occurs at the tool tip. It can be seen that the cutting edge changes and wears, and there is a phenomenon of micro edge collapse. With the progress of the machining process, the wear area of Wear II is further expanded. It can be seen from the three-dimensional graphics that the tool tip is further reduced, which is the result of more blade material peeling. The phenomenon of blade material peeling and micro edge collapse is more serious. For Wear III with the most serious wear, the tool tip has completely peeled off, and the wear area has further expanded along the flank, completely covering the cutting depth. Due to the complete peeling off of the tool tip, the height in the three-dimensional image is displayed more evenly. Through the analysis of end face wear and back face wear, the tool wear forms

in micro milling mainly include abrasion marks, built-up edges, micro-collapse blades, plastic deformation and delamination. In conclusion, with the progress of cutting, the wear area of the flank of the micro-milling cutter gradually expands, and the tool tip gradually peels off until it is completely peeled off, which seriously reduces the cutting performance of the micro-milling cutter.

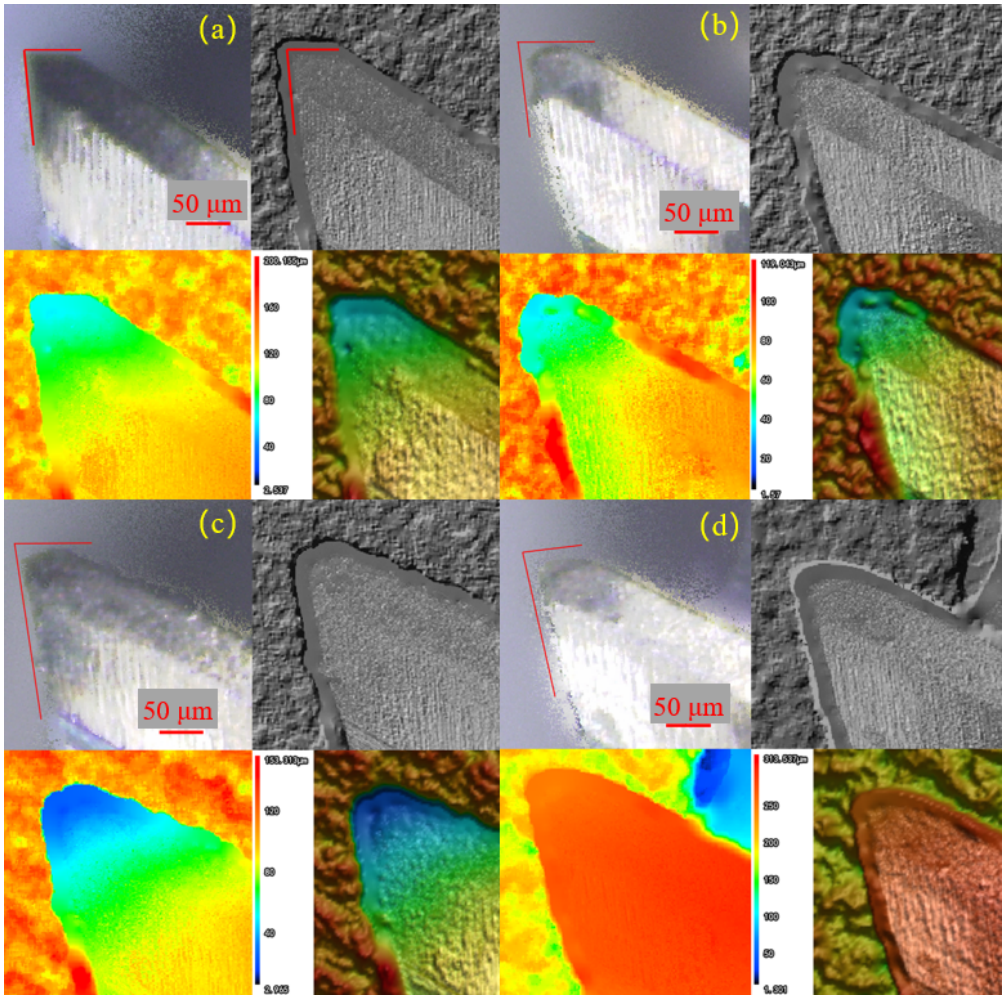

Figure 9. Analysis and three-dimensional topography of tool surface wear under different wear states. (**a**) Initial's confocal microscopic image, (**b**) Wear I's confocal microscopic image, (**c**) Wear II's confocal microscopic image and (**d**) Wear III's confocal microscopic image.

3.3. Edge Radius

As shown in Figure 10, the side image of the micro-milling cutter can more clearly and intuitively see the wear of the flank under different wear states. With the progress of the cutting process, the wear degree in both directions gradually increases until the tool tip completely peels off, which marks the end of the service life of the micro-milling cutter. With the wear and peeling of the tool tip, the edge radius obviously changes. As can be seen from Figure 8, the end face tip of the micro-milling cutter is highlighted with a yellow circle. With the development of wear, the tool tip obviously changes and the edge radius increases gradually, which is obtained from the comprehensive analysis of the end image and side image of the cutting edge. With the increase of the edge radius, the edge radius and the cutting depth are closer in order of magnitude and value, which is more obviously affected by the size effect, and the plowing effect will occur more frequently, or even completely replace the cutting effect. The increase of the edge radius seriously affects the cutting performance of the micro-milling cutter and increases the minimum

chip thickness. Under the condition of keeping the cutting parameters unchanged, it will produce the adverse results of difficult chip formation, plowing instead of cutting and a serious decline of surface quality.

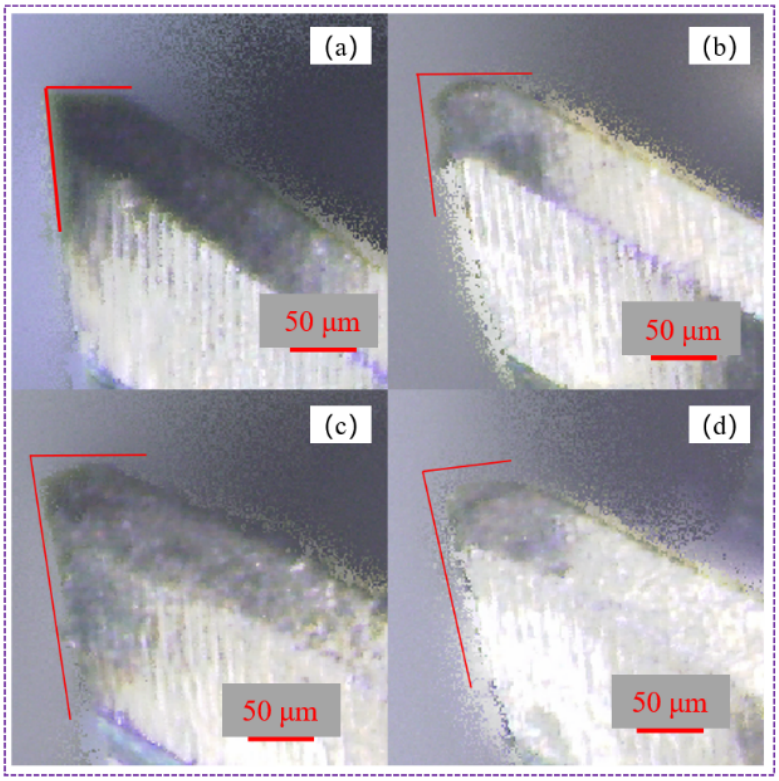

Figure 10. Wear analysis of micro milling cutters with different wear states. (**a**) Initial's flank wear profile, (**b**) Wear I's flank wear profile, (**c**) Wear II's flank wear profile and (**d**) Wear III's flank wear profile.

3.4. Tool Diameter Reduction

The images taken by the confocal laser microscope (Keyence, Osaka, Japan) and SEM are quantitatively described and analyzed by multi-file-analysis software (VK-X Series, Keyence, Osaka, Japan), and the wear amount of the end face is measured by a parallel-line ranging tool. The measurement scheme is described in the above section and the measurement results and average values of each cutting edge are shown in Figure 11. The material removal amount is calculated by the product of the machining path length, machining width and cutting depth. Because the single factor control experiment is adopted in this study, the cutting depth and cutting width are kept unchanged, and the amount of material removal is equivalent to the length of the machining path. It can be seen that there is little difference in the end-face wear between cutting edges, which is in line with the characteristics of end milling, and also shows the machining stability of the self-developed micro-milling platform from the side. The wear volume does not increase in a simple linear relationship, but gradually increases as the amount of material removed increases. This indicates that with the progress of the machining process, the tool wear rate is gradually accelerated, and the tool wear will promote the further wear of the tool. This is because the micro-milling process is a complex process with thermal mechanical coupling and a high strain rate. Tool wear changes the tool contact interface, changes the size and shape of the cutting edge, reduces the cutting performance and makes it easier to wear further.

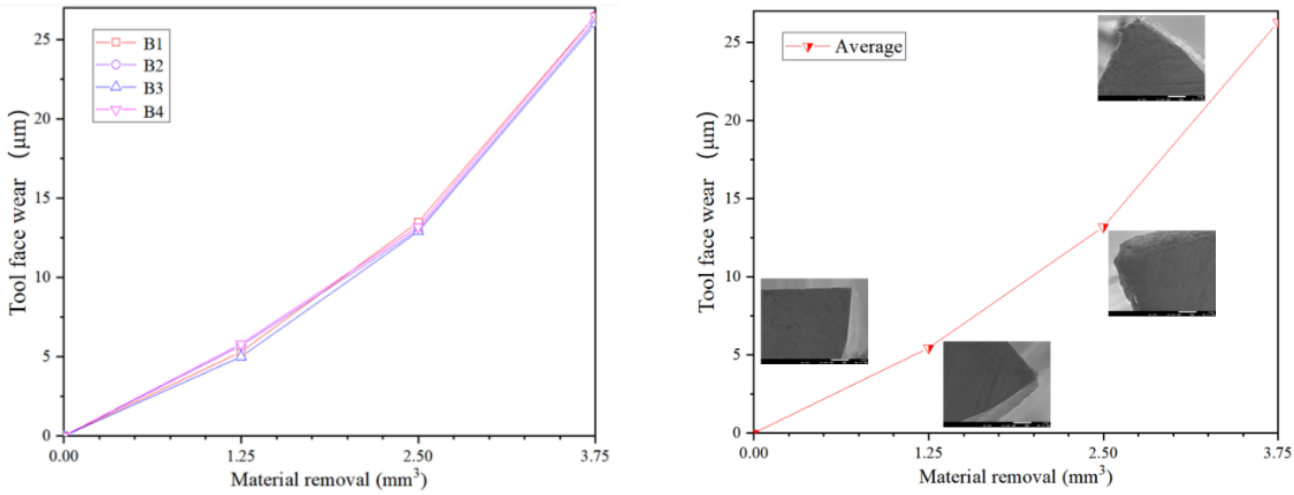

(**a**) (**b**)

Figure 11. Effect of material removal volume on tool face wear in micro milling Ti-6Al-4V. (**a**) Tool face wear of different cutting edges; (**b**) the average amount of tool face wear.

The amount of flank wear is also quantitatively analyzed by parallel line ranging and other tools in multi-file-analysis software. The analysis results are shown in Figure 12. Different from the end face wear, the wear amount on the side of each cutting edge is significantly different. This may be caused by the different strengths of each cutting edge in the side direction determined by the structure of the micro-milling cutter. It may also be caused by the instability of the processing environment, such as machine tool vibration caused by the environment. The wear law is similar to the end face wear. The early stage belongs to the stable wear stage and the wear rate is low. With the micro-milling cutter in Wear II, the wear rate increases significantly, indicating that the cutter enters the rapid wear stage. Due to the different strengths of the end face and side tool, the difference of flank wear in the wear rate is more obvious.

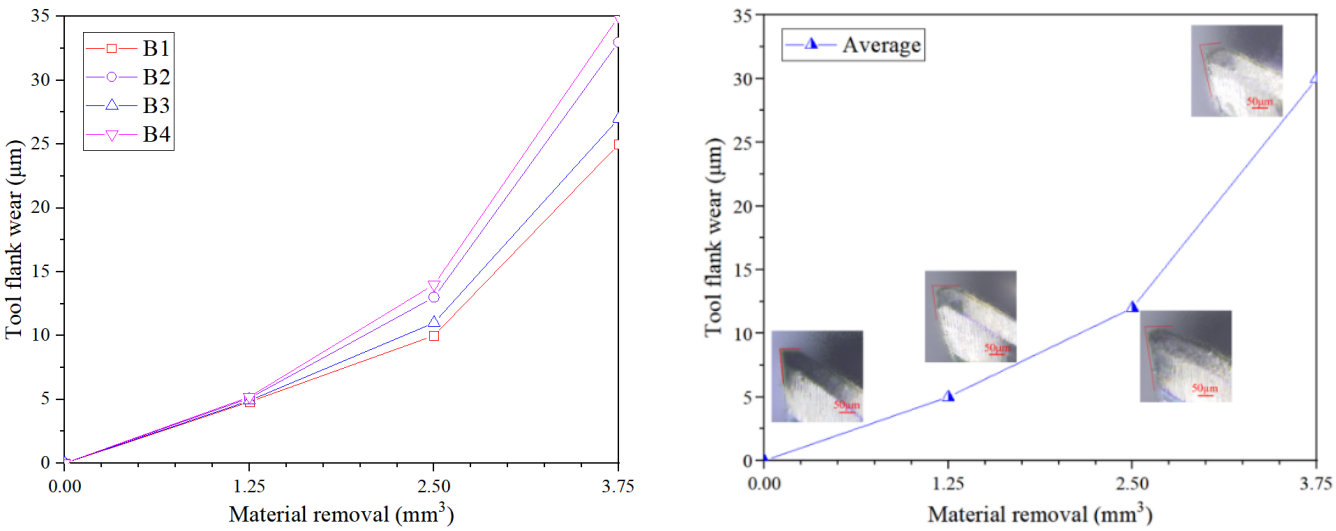

(**a**) (**b**)

Figure 12. Effect of material removal volume on tool flank wear in micro milling Ti-6Al-4V. (**a**) Tool flank wear of different cutting edges; (**b**) the average amount of tool flank wear.

Micro-milling cutters are generally used in the machining condition of the end milling groove, so the change of edge diameter has a close impact on the machining surface quality. The research results of other scholars show that the edge diameter and edge height are essential to the analysis of the wear state of micro-milling cutters. The analysis results of

edge diameter and edge height of a micro-milling cutter in different wear states are shown in Figure 13. The starting point of diameter measurement selects the inner position of the tool tip peeling and the distance measurement tool between two points in VK-X software (Keyence, Osaka, Japan) is used for measurement. With the progress of machining, the tool is gradually worn, which is realized as the gradual reduction of edge diameter and edge height. With the wear of the tool, the wear rate increases gradually, which is similar to the wear law of the end face and flank.

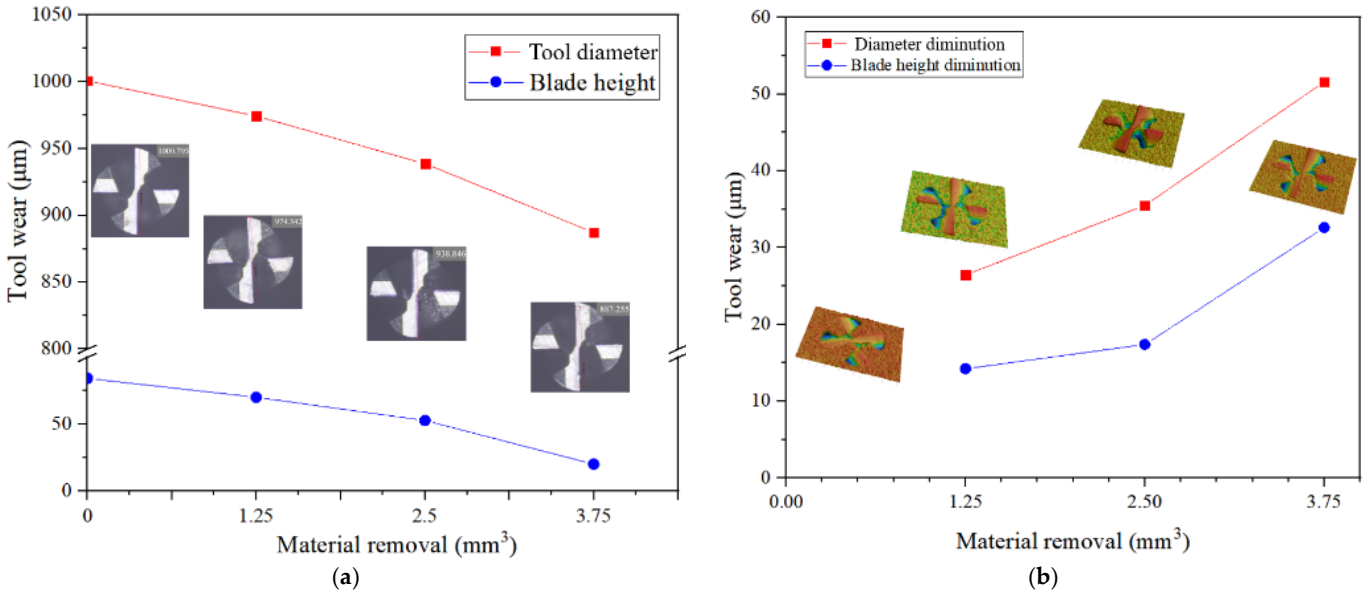

Figure 13. Effect of material removal on micro milling cutter wear. (**a**) Change of tool diameter and blade height; (**b**) change of tool diameter diminution and blade height diminution.

3.5. Tool Wear Mechanisms

Micro-milling Ti-6Al-4V tool wear mainly occurs at the tool tip, and a variety of wear forms occur at the same time. Adhesive wear is the main cause of tool wear. The damage mechanisms of a micro-milling tool under low speed conditions are mainly abrasive wear and adhesive wear. When the cutting speed increases, adhesive wear occurs, and there is a certain degree of oxidative wear at the tool tip. As shown in Figure 14, the wear phenomena of micro-milling cutters in different wear states are marked. Among them, the surface of the cutting edge of the new tool is smooth and flat. Due to the short processing path, low wear degree and the less adhesive material, Ti-6Al-4V, only slight tool material peeling occurs. It shows that the degree of adhesive wear is small and the influence on the cutting edge is limited. With the further deepening of the wear degree, a large number of BUE appear in Wear II, and some bare cutting edge surfaces are clearly visible. It can be seen from the previous analysis that the BUE in dynamic change is extremely unstable and easily peels off and takes away tool material, resulting in further wear of the tool. With the progress of cutting, the severe tool wear further increases the cutting temperature, and the local high temperature and stress concentration are more serious. Therefore, the loose pore structure caused by micro molten Ti-6Al-4V and the intergranular degumming of tool material can be observed on the tool surface in Wear III. The less adherent material Ti-6Al-4V was found, which does not indicate an improvement in the wear state. Rather, severe tip spalling was observed because of BUE spalling under long-term dynamic action, taking away material from the cutting edge. The energy spectrum of each micro-milling cutter is obtained through EDS, and the results are shown in Figure 15. The Ti content of a micro-milling cutter in four wear states is 0%, 3.4%, 4% and 3.7%, respectively. With the progress of the machining process, more and more workpiece materials adhere to the cutting edge, which proves the previous conclusion. In particular, the Ti content decreases in the process from Wear II to Wear III. This is because BUE is composed of accumulated

workpiece material Ti-6Al-4V. The dynamic action makes BUE peel off, which makes the phenomenon of the Ti content decrease in Wear III, which does not affect the previous conclusion. This corresponds to Figure 14d, and the spalling of BUE can be clearly observed. Combined with SEM and EDS, the adhesive wear process and mechanism in the machining process are analyzed. It is found that adhesive wear accompanies the whole cutting process and plays a major role.

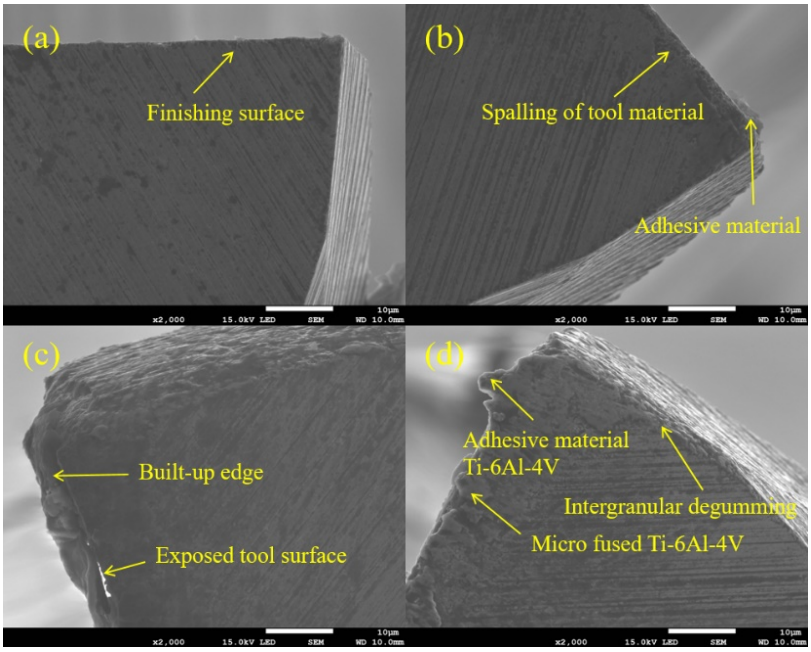

Figure 14. SEM microscopic images of micro-milling cutter under different wear states. (**a**) Initial's SEM image and wear form, (**b**) Wear I's SEM image and wear form, (**c**) Wear II's SEM image and wear form and (**d**) Wear III's SEM image and wear form.

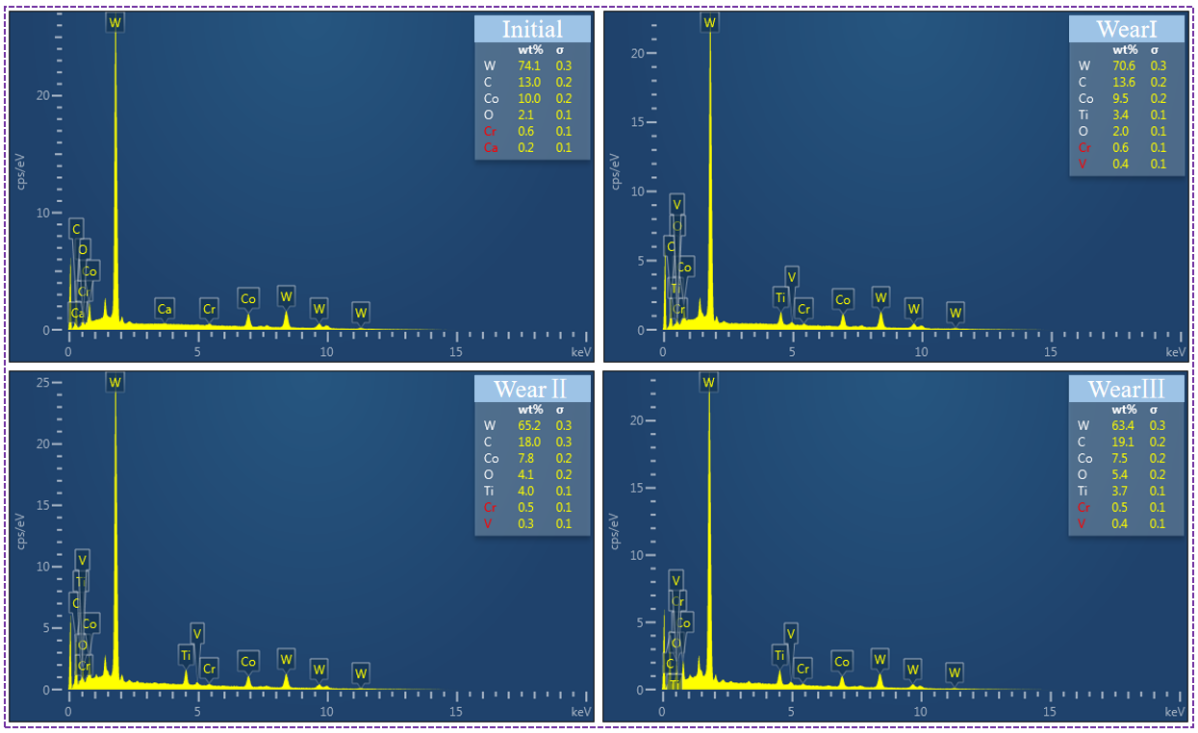

Figure 15. EDS analysis of micro-milling cutter with different wear states.

The melting point of Co is low, and it will soften under the action of high cutting heat, resulting in the peeling off of WC particles. The appearance of micro molten Ti-6Al-4V shows that the local temperature is high during cutting, and the high temperature leads to the peeling of tool materials at the same time. Therefore, intergranular degumming can be observed, which is why they are often observed at the same time. The Co content of a micro-milling cutter in four wear states is 10%, 9.5%, 7.8% and 7.5%, respectively. Co shows a gradual decrease, which proves that with the increase of the cutting temperature, the softening of binder leads to the loss and peeling of WC particles of workpiece material, and the separation of WC particles from binder are the main causes of abrasive wear. Local high temperature and chemical element concentration gradient make it possible for element dissolution and diffusion. In high-speed milling, the high temperature generated in the chip friction zone (SDZ) intensifies the dissolution and diffusion of elements at the interface. From Figure 14d, the micro melting Ti-6Al-4V and intergranular degumming indicate the generation of local high temperature in the cutting process, and the energy spectrum also indicates the loss of tool material and the gradual increase of workpiece material on the tool. From Figure 15, it can be seen that the V element content of a micro-milling cutter in four wear states is 0%, 0.1%, 0.3% and 0.4%, respectively, and the Cr element content is 0.6%, 0.6%, 0.5% and 0.5%, respectively. The increase of V and the decrease of Cr in the elements contained in the tool also prove the existence of dissolution and diffusion wear. However, these phenomena are not observed in Figure 14a–c, indicating that at the initial stage of wear, the cutting temperature does not reach the critical temperature of element dissolution and diffusion, and dissolution and diffusion wear do not occur. During the micro-milling process, the local increase of the cutting temperature will provide conditions for a chemical reaction between the tool material WC, the adhering material Ti-6Al-4V and the environment (mainly oxygen), thereby further aggravating tool wear. Figure 16 shows the element distribution and SEM micro image of the wear area of the cutting edge. The local SEM images of the tool tip under different wear states can clearly see the change of the edge radius, which further proves that the tool wear makes the edge radius gradually increase. The results show that the O element content of micro-milling cutters in four different wear states is 2.1%, 2%, 4% and 5.4%, respectively. The increase of O element content confirms the strong oxidation reaction on the tool surface. At the initial stage of wear, the oxygen content of the Wear I micro-milling cutter is consistent with that of the new cutter, which indicates that the oxidation reaction conditions are not reached and there is no oxidation reaction. From Wear II, due to the improvement of wear degree, a higher local cutting temperature is produced and the reaction conditions are reached, so a strong oxidation reaction occurs. The high enrichment of the O element near the cutting edge is mainly due to the convenient penetration of oxygen in the air during the cutting process. WC easily reacts with Ti and O under high-temperature conditions, and the binder Co is also very easy to oxidize to Co_3O_4. Therefore, oxidative wear intensifies the failure of the binder and the peeling of tool particles, which has an adverse impact on the cutting performance of a micro-milling cutter.

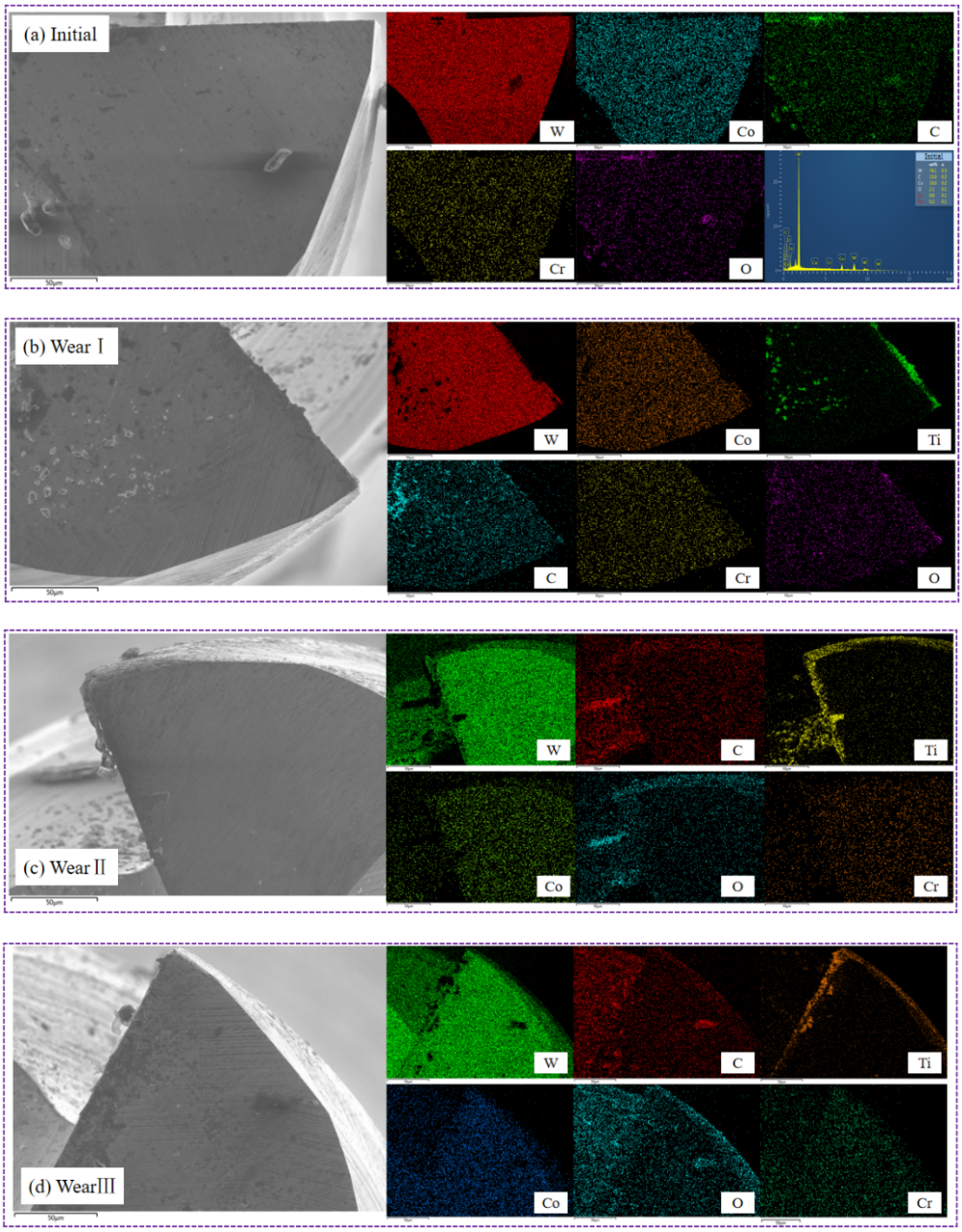

Figure 16. SEM/EDS data of micro milling cutter under different wear states. (**a**) Element distribution of Initial; (**b**) Element distribution of Wear I; (**c**) Element distribution of Wear II; (**d**) Element distribution of Wear III.

4. Conclusions

To study the wear process and wear mechanism of micro-milling cutters with different wear states, an experimental scheme for milling Ti-6Al-4V with WC carbide micro-milling cutters was designed. Four micro-milling cutters with different wear states were obtained and the data of the micro-milling cutters were collected. Confocal laser images, SEM images and EDS images were obtained and studied. The wear-failure standard, wear process and wear mechanism of micro-milling cutters are comprehensively analyzed. The formulation of a wear standard and the disclosure of the wear mechanism provide theoretical data support for the application and popularization of micro milling in the field of difficult-to-machine materials. The key findings of this experimental research work include the following:

1. The wear modes are classified into progressive normal wear failure and abnormal wear failure. The progressive normal wear failure mainly includes abrasion marks, material adhesion, built-up edges (BUE) and micro-blade collapse, while the abnormal wear failure mainly includes severe plastic deformation, blade collapse, catastrophic fracture and delamination of the cutting edge. Due to the micron size, the influence of BUE is amplified and plays a leading role in cutting performance.
2. There is no relevant international standard for the wear of a micro-milling cutter. According to the characteristics of micro milling, a comprehensive analysis was conducted from the aspects of end face wear, flank wear, edge diameter reduction and edge radius. The wear of end face 30 μm, wear of flank 35 μm and tool diameter reduction 55 μm can be used as the failure criteria of a micro-milling cutter. Tool wear makes the edge radius increase gradually, which seriously affects the cutting performance of a micro-milling cutter.
3. The wear process and wear mechanism of micro-milling cutter machining are analyzed. Adhesive wear exists in the whole cutting process and plays a major role. High temperature, element concentration gradient and oxygen provide conditions for abrasive particle shedding, element diffusion and oxidation reaction. Abrasive wear, diffusion wear and oxidation wear occur only when the cutting temperature reaches the melting point of Co, and oxidation wear aggravates the failure of the binder and the peeling off of tool particles.

Author Contributions: Conceptualization, Q.S.; methodology, T.Z.; Software, T.Z.; formal analysis, T.Z.; investigation, T.Z.; resources, Q.S.; data curation, T.Z.; writing—original draft preparation, T.Z.; writing—review and editing, T.Z.; supervision, Z.L.; project administration, Y.D.; funding acquisition, Q.S. All authors have read and agreed to the published version of the manuscript.

Funding: This research was funded by the National Natural Science Foundation of China, grant numbers 51875320 and 51922066, and the Natural Science Foundation of Shandong Province, grant numbers ZR2019JQ19 and 2019JMRH0307.

Institutional Review Board Statement: Not applicable.

Informed Consent Statement: Not applicable.

Data Availability Statement: All the data are available within the manuscript.

Conflicts of Interest: The authors declare no conflict of interest.

References

1. Hoyle, R. Developments in micro and nano engineering and manufacturing. *Plas. Rub. Comp.* **2008**, *37*, 50–56. [CrossRef]
2. Dhanorker, A.; Ozel, T. Meso/micro scale milling for micro-manufacturing. *Int. J. Mech. Manuf. Syst.* **2008**, *1*, 23–42. [CrossRef]
3. Iqbal, A.; Zhao, G.; Zaini, J.; Gupta, M.K.; Jamil, M.; He, N.; Nauman, M.M.; Mikolajczyk, T.; Pimenov, D.Y. Between-the-holes cryogenic cooling of the tool in hole-making of Ti-6Al-4V and CFRP. *Materials* **2021**, *14*, 795. [CrossRef]
4. Sen, B.; Gupta, M.K.; Mia, M.; Pimenov, D.Y.; Mikołajczyk, T. Performance assessment of minimum quantity castor-palm oil mixtures in hard-milling operation. *Materials* **2021**, *14*, 198. [CrossRef] [PubMed]
5. Jamil, M.; Khan, A.M.; Hegab, H.; Gong, L.; Mia, M.; Gupta, M.K. Effects of hybrid Al_2O_3-CNT nanofluids and cryogenic cooling on machining of Ti–6Al–4V. *Int. J. Adv. Manuf. Technol.* **2019**, *102*, 3895–3909. [CrossRef]
6. Pimenov, D.Y.; Mia, M.; Gupta, M.K.; Machado, A.R.; Tomaz, I.V.; Sarikaya, M.; Wojciechowski, S.; Mikolajczyk, T.; Kaplonek, W. Improvement of machinability of Ti and its alloys using cooling-lubrication techniques: A review and future prospect. *J. Mater. Res. Technol.-JMRT.* **2021**, *11*, 719–753. [CrossRef]
7. Adebiyi, D.I.; Popoola, A.P.I. Mitigation of abrasive wear damage of Ti-6Al-4V by laser surface alloying. *Mater. Des.* **2015**, *74*, 67–75. [CrossRef]
8. Wang, C.Y.; Xie, Y.X.; Qin, Z.; Lin, H.S.; Yuan, Y.H.; Wang, Q.M. Wear and breakage of TiAlN-and TiSiN-coated carbide tools during high-speed milling of hardened steel. *Wear.* **2015**, *336*, 29–42. [CrossRef]
9. Aslantas, K.; Hopa, H.E.; Percin, M.; Ucun, I.; Çicek, A. Cutting performance of nano-crystalline diamond (NCD) coating in micro-milling of Ti6Al4V alloy. *Precis. Eng.* **2016**, *45*, 55–66. [CrossRef]
10. International Standards Organisation. *ISO 8688-1*; Tool Life Testing in Milling—Part 1: Face Milling. ISO: Geneva, Switzerland, 1989.

11. International Standards Organisation. *ISO 8688-2*; Tool Life Testing in Milling—Part 2: End Milling. ISO: Geneva, Switzerland, 1989.
12. Lai, X.; Li, H.; Li, C.; Lin, Z.; Ni, J. Modelling and analysis of micro scale milling considering size effect, micro cutter edge radius and minimum chip thickness. *Int. J. Mach. Tools. Manuf.* **2008**, *48*, 1–14. [CrossRef]
13. Liu, X.; Devor, R.E.; Kapoor, S.G. An analytical model for the prediction of minimum chip thickness in microm-achining. *J. Manuf. Sci. Eng.* **2006**, *128*, 474–481. [CrossRef]
14. Zhu, K.; Yu, X. The monitoring of micro milling tool wear conditions by wear area estimation. *Mech. Syst. Sign. Pro.* **2017**, *93*, 80–91. [CrossRef]
15. Alhadeff, L.L.; Marshall, M.B.; Curtis, D.T.; Slatter, T. Protocol for tool wear measurement in micro-milling. *Wear* **2018**, *420*, 54–67. [CrossRef]
16. Han, J.J.; Ma, R.; Hao, X.Q.; Kong, L.L.; Chen, N. Experimental research on deep-and-narrow micromilled grooves using a self-fabricated PCD micro-cutter. *Micromachines* **2021**, *12*, 1170. [CrossRef]
17. Manso, C.S.; Thom, S.; Uhlmann, E.; Assis, C.L.F.; Conte, E.G. Tool wear modelling using micro tool diam-eter reduction for micro-end-milling of tool steel H13. *Int. J. Adv. Manuf. Technol.* **2019**, *105*, 2531–2542. [CrossRef]
18. Ziberov, M.; Da Silva, M.B.; Jackson, M.; Hung, W.N.P. Effect of cutting fluid on micromilling of Ti-6Al-4V titanium alloy. *Procedia Manuf.* **2016**, *5*, 332–347. [CrossRef]
19. Dadgari, A.; Huo, D.; Swailes, D. Investigation on tool wear and tool life prediction in micro-milling of Ti-6Al-4V. *Nano-Technol. Precis. Eng.* **2018**, *1*, 218–225. [CrossRef]
20. Oliaei, S.N.; Karpat, Y. Influence of tool wear on machining forces and tool deflections during micro milling. *Int. J. Adv. Manuf. Technol.* **2015**, *84*, 1963–1980. [CrossRef]
21. Silva, E.L.; Pratas, S.; Neto, M.A.; Fernandes, C.M.; Figueiredo, D. Multilayer diamond coatings applied to micro-end-milling of cemented carbide. *Materials* **2021**, *14*, 3333. [CrossRef]
22. Muhammad, A.; Kumar Gupta, M.; Mikołajczyk, T.; Pimenov, D.Y.; Giasin, K. Effect of tool coating and cutting parameters on surface roughness and burr formation during micromilling of inconel 718. *Metals* **2021**, *11*, 167. [CrossRef]
23. Wang, Y.; Zou, B.; Wang, J.; Wu, Y.; Huang, C. Effect of the progressive tool wear on surface topography and chip formation in micro-milling of Ti–6Al–4V using Ti(C7N3)-based cermet micro-mill. *Tribol. Int.* **2020**, *141*, 105900. [CrossRef]
24. Sahoo, P.; Patra, K.; Pimenov, D.Y. Enhancement of micro milling performance by abrasion-resistant coated tools with optimized thin-film thickness: Analytical and experimental characterization. *Int. J. Adv. Manuf. Technol.* **2022**. [CrossRef]
25. Varghese, A.; Kulkarni, V.; Joshi, S.S. Tool life stage prediction in micro-milling from force signal analysis using machine learning methods. *ASME J. Manuf. Sci. Eng.* **2020**, *143*, 054501. [CrossRef]
26. Saha, S.; Deb, S.; Bandyopadhyay, P.P. Progressive wear based tool failure analysis during dry and MQL assisted sustainable micro-milling. *Int. J. Mech. Sci.* **2021**, *212*, 106844. [CrossRef]
27. Jaffery, S.H.I.; Mativenga, P.T. Wear mechanisms analysis for turning Ti-6Al-4V-towards the development of suita-ble tool coatings. *Int. J. Adv. Manuf. Technol.* **2012**, *58*, 479–493. [CrossRef]
28. Sarıkaya, M.; Gupta, M.K.; Tomaz, I.; Pimenov, D.Y.; Kuntoğlu, M.; Khanna, N.; Yıldırım, Ç.V.; Krolczyk, G.M. A state-of-the-art review on tool wear and surface integrity characteristics in machining of superalloys. *CIRP J. Manuf. Sci. Technol.* **2021**, *35*, 624–658. [CrossRef]
29. Thakur, D.G.; Ramamoorthy, B.; Vijayaraghavan, L. Some investigations on high speed dry machining of aerospace material Inconel 718 using multicoated carbide inserts. *Adv. Manuf. Prof.* **2012**, *10*, 1066–1072. [CrossRef]
30. Qi, G.; Guangyan, G.; Ming, C. Wear mechanism and experimental study of a tool used for micro-milling sin-gle-crystal nickel-based superalloys. *Int. J. Adv. Manuf. Technol.* **2021**, *113*, 117–129. [CrossRef]
31. Zhang, J.F.; Feng, C.; Wang, H.; Gao, Y.D. Analytical investigation of the micro groove surface topography by micro-milling. *Micromachines* **2019**, *10*, 582. [CrossRef]
32. Aslantas, K.; Ülker, Ş.; Şahan, Ö.; Pimenov, D.Y.; Giasin, K. Mechanistic modeling of cutting forces in high-speed microturning of titanium alloy with consideration of nose radius. *Int. J. Adv. Manuf. Technol.* **2022**, *119*, 2393–2408. [CrossRef]